Thin Solid Films 685 (2019) 366–371

Contents lists available at ScienceDirect

Thin Solid Films

journal homepage: www.elsevier.com/locate/tsf

Highly conductive and smooth surfaced flexible transparent conductive electrode based on silver nanowires

Mahesh A. Shinde[a], Dong-Jun Lee[b], Byoung-Joon Kim[b,*], Haekyoung Kim[a,*]

[a] School of Materials Science and Engineering, Yeungnam University, Gyeongsan-si 38541, Republic of Korea
[b] School of Materials Science and Engineering, Andong National University, Andong-si 36729, Republic of Korea

ARTICLE INFO

Keywords:
Silver
Nanowire
Metal mesh
Flexible substrate
Transparent conductive electrode
Surface roughness
Stability
Imprinting

ABSTRACT

Silver nanowires (AgNWs) based conductive electrode have shown potential for use in large area flexible optoelectronic applications. Presently, considerable efforts are being made to lower the surface roughness and enhance the opto-electrical performance of AgNWs based transparent conductive electrode(TCE) for optoelectronic application, which require a smooth surface for high efficiency performance. In this work, we designed a hybrid metal electrode with low surface roughness fabricated by coating an AgNWs onto a metal mesh on Polyethylene terephthalate substrate (AgNW/MM/PET). The AgNW/MM/PET TCE, fabricated by a method of hot pressing after wire wound-rod coating process, exhibits a low surface roughness of 8 nm and 16.33 nm of maximum peak-to-valley value with the low sheet resistance of 0.668 Ω/sq. and a high optical transmittance of 91.25% at λ = 550 nm. In addition, the hot pressed AgNW/MM/PET TCE shows excellent mechanical stability along with long-term reliability in bending tests and strong adhesion in taping test, compared to the annealed AgNW/MM/PET TCE. Therefore, the hot pressed AgNW/MM/PET electrodes with low surface roughness and high opto-electrical performance could be a potential candidate to replace indium doped tin oxide electrodes in flexible electronic application.

1. Introduction

A transparent conducting electrode (TCE) is a widely used in development and fabrication of flexible optoelectronic application, like liquid-crystal displays, touch screen, thin-film transistors, organic light-emitting diodes (OLEDs), and solar cells [1–5]. The development of highly conductive TCE is a very important issue especially for the large area electronic devices such as large size display or smart windows. If the resistance of TCE is not sufficiently low, the delay in operation will be occurred according to the different distance from the input terminal. The opto-electric properties of TCE enable to extraction of electrical charge along with light transmission [6]. The indium tin oxide (ITO) is the most commonly used transparent conductor owing to its opto-electric performance(sheet resistance- 10–20 Ω/sq. and optical transmittance up to 85%) [7–9]. However, its costly deposition systems, high cost and inherent brittleness limit its applicability in TCEs [10,11]. Various materials have been studyed for replacement of ITO, like metal nanowires [12–16], carbon nanotubes [17], graphene [18], conductive polymers [19], and metal meshes [20,21]. Metal nanowires are most often considered as a possible replacement for ITO in flexible optoelectronic devices because of its high opto-electric performance and tunable figure of merit. Specifically, silver nanowire (AgNWs) have been demonstrated as most favorable material for flexible TCEs due to their admirable mechanical and opto-electrical properties (sheet resistance ~10 Ω/sq. at 90% transmittance). However, it is still difficult to improve the conductivity of AgNWs electrode with maintaining transmittance over more than 90% [22]. Metal mesh on Polyethylene terephthalate substrate (MM/PET) TCE also a favorable alternative due to its ability to easily control its opto-electrical performance by varying the thickness, spacing and width of grid [23]. The MM/PET also enable continuous pathway for an electric carrier in metal grid lines crossing one another, which make it low junction resistance structure [24]. In spite of these all advantages, there are some practical problem in AgNWs and MM/PET electrodes like surface roughness, which limit their use in organic electronic devices. On a TCE there are certain junctions where more than one AgNWs are stacked on one another which results increasing maximum peak-to-valley values of TCE by two or three times the diameter of the nanowires [25,26]. In generally for fabrication of TCE the nanowires with a diameter of 90 nm are used. Therefore, when at a certain junction if three nanowire are stacked on top of each other the maximum peak-to-valley value will be become 270 nm, which makes it quite problematic for device applications. In

* Corresponding authors.
E-mail addresses: bjkim@anu.ac.kr (B.-J. Kim), hkkim@ynu.ac.kr (H. Kim).

https://doi.org/10.1016/j.tsf.2019.06.054
Received 29 January 2019; Received in revised form 27 June 2019; Accepted 28 June 2019
Available online 29 June 2019
0040-6090/ © 2019 Elsevier B.V. All rights reserved.

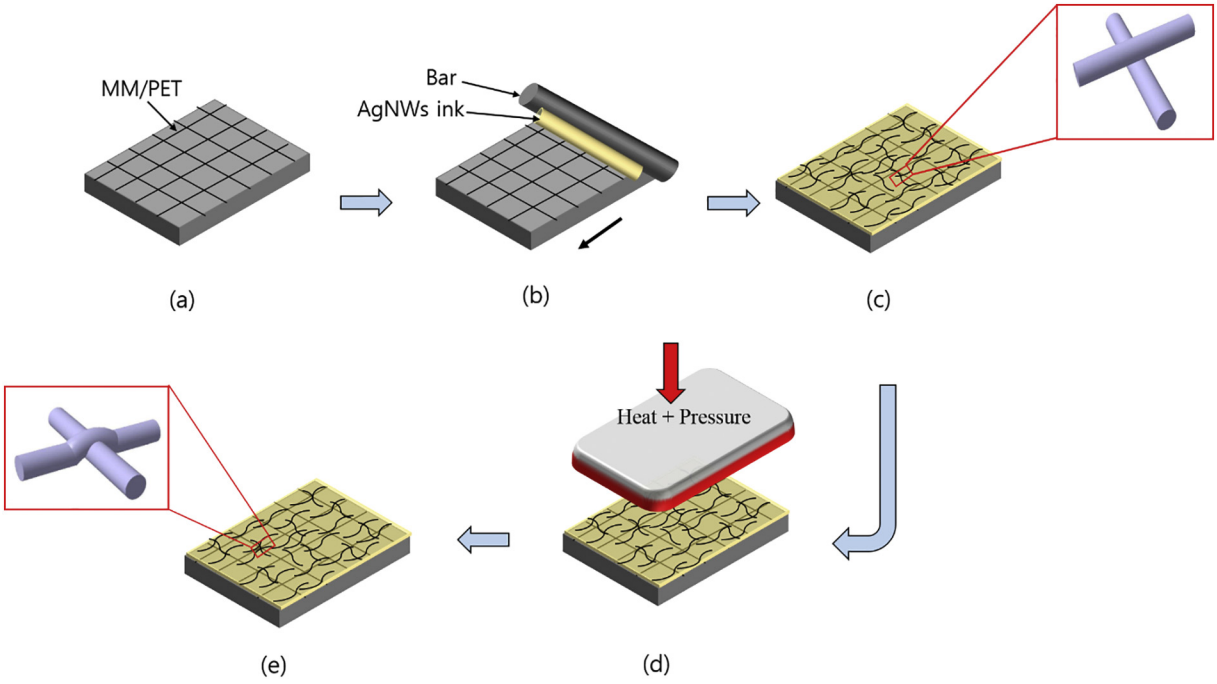

Scheme 1. Transparent conductive electrode fabrication procedure; a) MM/PET, b) Bar coating on MM/PET, c) Room-temperature drying with bird's eye view of stacked nanowire, (d) Hot pressing, (e) Fabricated AgNW/MM/PET with bird's eye view of welded nanowire junction.

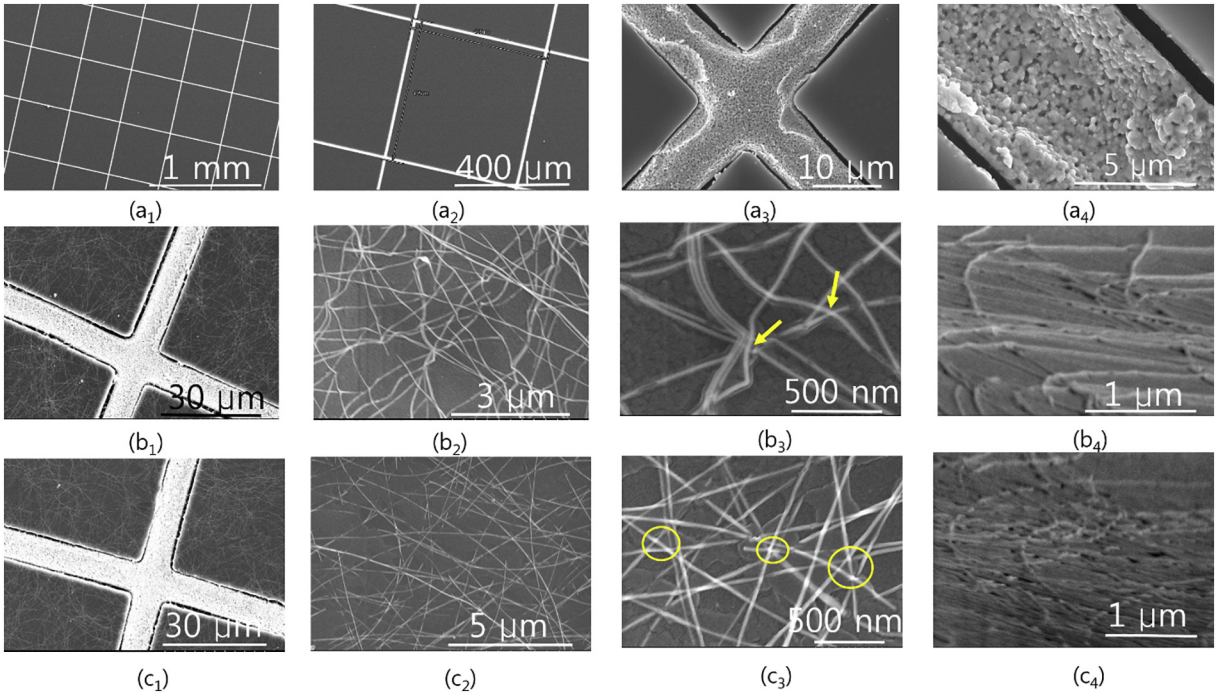

Fig. 1. ($a_{1–4}$) SEM images of the MM structure-patterned on the PET substrate, ($b_{1–4}$) SEM images of the annealed AgNW/MM/PET TCE, and ($c_{1–4}$) SEM images of the hot pressed AgNW/MM/PET TCE.

solar cell the high surface roughness cause to increase dark current, which results lower efficient of solar cell [27–29]. In OLEDs, the rough TCE surfaces cause increase in leakage of current, which resulting failure of device [30].

Many works have been reported to solve surface roughness problem for TCE. In the previous work, the researcher used a conductive polymer layer on a nanowire electrode to decrease surface roughness, which eventually lower the efficiency and transparency of the device [26].

In some cases, researchers used non-conductive polymers, which caused a greater increase in the transmittance of TCE than conductive polymer. However, use of the non-conducting makes the TCE fabrication method more difficult [31]. In addition, a few earlier studies preferred pressing as a method for TCE fabrication. Tokuno et al. [32] pressed AgNWs film mechanically at room temperature that results 18 nm surface roughness of TCE, which is still high. Hauger et al. [33] hot pressed AgNW film, which results12 nm surface roughness of TCE. Yu et al. [34] hot pressed AgNWs on glass substrate. The achieved

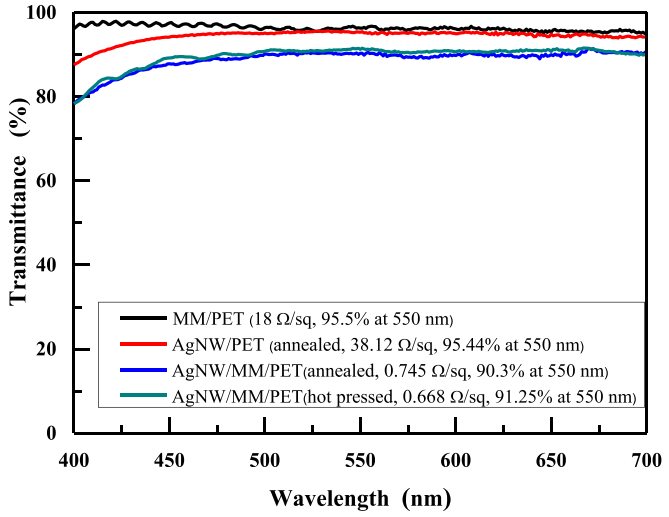

Fig. 2. Transmission over the wavelength of 400–700 nm with a sheet resistance of annealed AgNW/PET, MM/PET, annealed and hot pressed AgNW/MM/PET TCE.

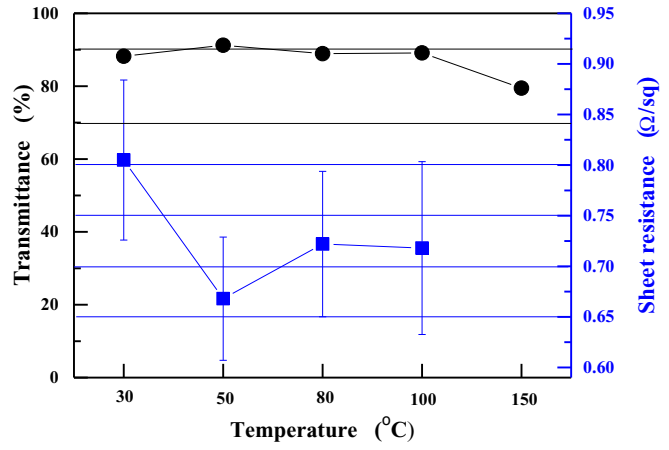

Fig. 3. Sheet resistance and the optical transmittance of the AgNW/MM/PET TCE that was pressed (10 MPa) at different temperatures.

roughness was 11.7 nm and the maximum peak-to-valley value was 40 nm. Chen et al. [35] hot-press transfer of graphene monolayer on AgNWs electrode, which make fabrication of TCE difficult. Several works addressed various techniques to solve roughness problems of the TCE. However, very less work reported regarding maximum peak-to-valley value of the electrode, which is also an essential factor in dealing with electrical shorts in optoelectronic devices.

In this work, a simple and low cost method to enhance the optoelectric properties and lower the surface roughness of the AgNW/MM/PET TCE was proposed. Low-resistance TCE was developed via hybridization of MM/PET and AgNWs. A smooth surface was obtained using a hot press on AgNWs electrode, which also prevented damage of pre-processed MM/PET electrode. AgNWs were coated onto the MM/PET TCE and after coating sequentially, a hot pressing process was applied to the hybrid electrode. After the hot pressing, the stacked AgNWs was found to be joined together owing to thermo-mechanical pressure, and there was an enhancement in sheet resistance (0.668 Ω/sq) along with good optical transmittance (91.25% at λ = 550 nm). The achieved Root Mean Square (RMS) surface roughness and maximum peak-to-valley value of the hot pressed AgNW/MM/PET TCE was 8 and 16.33 nm, respectively. This result was achieved without use of any additional materials, which fill the spaces between the nanowires. Furthermore, the hot pressed AgNW/MM/PET TCE exhibited excellent stability in a bending test and strong adhesion in a taping test, compared to the conventionally annealed AgNW/MM/PET TCE.

2. Experimental

AgNW ink (Active grid, C3nano) with nanowire having length of 20–30 μm and diameter of 45–60 nm were used. MM/PET TCE was fabricated by imprinting method on a Polyethylene terephthalate (PET) substrate, which was obtained from JUSUNG Engineering Co. The thickness of MM/PET substrate was ~ 150 μm and the width and the length of the metal (silver) mesh were ~ 10 and ~ 500 μm, respectively.

Scheme 1 shows the fabrication process of transparent conducting electrode. First, the AgNWs ink was stirred for 2–3 min. Later, the AgNWs was coated onto the MM/PET substrate (3 × 4 cm) by using a wire wound-rod coating prosess [36,37]. The thickness, uniformity and agglomeration of coated AgNWs film is control by distance between the coating wire wound-rod and substrate, and speed of the coating [38]. For coating, we used RDS24 bar and test 1 speed. The fabricated film was dried for 15 min at room temperature. The nominal wet coating thickness of prepared sample was ~61 μm. After coating, the AgNW/MM/PET TCE was hot pressed at a pressure of 10 MPa and a temperature of 50 °C for 4 min in a mechanical press (HMM-04 A, HANSUNG SYSTEMS, INC). As reference samples, AgNW/PET and the AgNW/MM/PET TCE were annealed in oven at 100 °C for 10 min, which is the general way to prepare a TCE.

A spectrophotometer (GENESYS 10S UV–vis, thermo scientific) and a four-probe technique (Loresta EP MCP-T360) were used to measure the optical and electrical properties, respectively. The microstructure of the AgNWs was observed by scanning electron microscopy (SEM) (S-4800, HITACHI, LTD with an acceleration voltage of 5 kV. Atomic force microscopy: all C-AFM measurements were carried out with a commercial AFM (XE 100, Park Systems Corp., Korea) under ambient conditions operating in contact mode using conductive AFM probes. The cantilevers have nominal spring constants of 0.2 N m^{-1}. The tape testing method was used to study the adhesion properties. 3 M tape was attached to the AgNW/MM/PET film, pressed it with a finger, and then peeled it off.

The mechanical property of the AgNWs was investigated by a simple bending test and a bending fatigue test using a U-bending test system (Bending tester, CKSI, Korea). The in situ electrical resistance of the samples were monitored by gripping them between two rotating conducting grips. The bending deformation of the AgNWs sample was introduced by changing the distance between the two plates. The applied strains were calculated by using the curvature relation $\varepsilon = \frac{hs}{2r}$ where hs is the substrate thickness and r is radius of curvature [39,40]. For the simple bending test, the bending radius was varied from 2 to 12 mm, which corresponds 3.125% and 0.52%, respectively. The fatigue test was conducted by repeatedly bending and unbending of the AgNWs, changing the gap between two guide plates. The bending radius was fixed at 5 mm, which corresponded to an applied strain of 1.25%. The motion length and the testing frequency were 60 mm and 1 Hz, respectively.

3. Results and discussion

The morphologies of TCEs were studied by SEM analyses. Fig. 1 illustrate the SEM images of the MM/PET, the annealed and hot pressed AgNW/MM/PET TCEs. The Fig. 1(a_{1-4}) shows morphologies of the silver grid pattern of the MM/PET TCE. From the morphology of the MM/PET TCE, the width and pitch of grid was found to be ~10 μm and ~500 μm, respectively. Fig. 1(b_{1-4}) and (c_{1-4}) show the morphologies of the annealed and hot pressed AgNW/MM/PET TCEs. Upon examining these figures, it was clearly seen that randomly oriented AgNWs were filled the space between the grids on the MM/PET TCE. Fig. 1(b_4) and

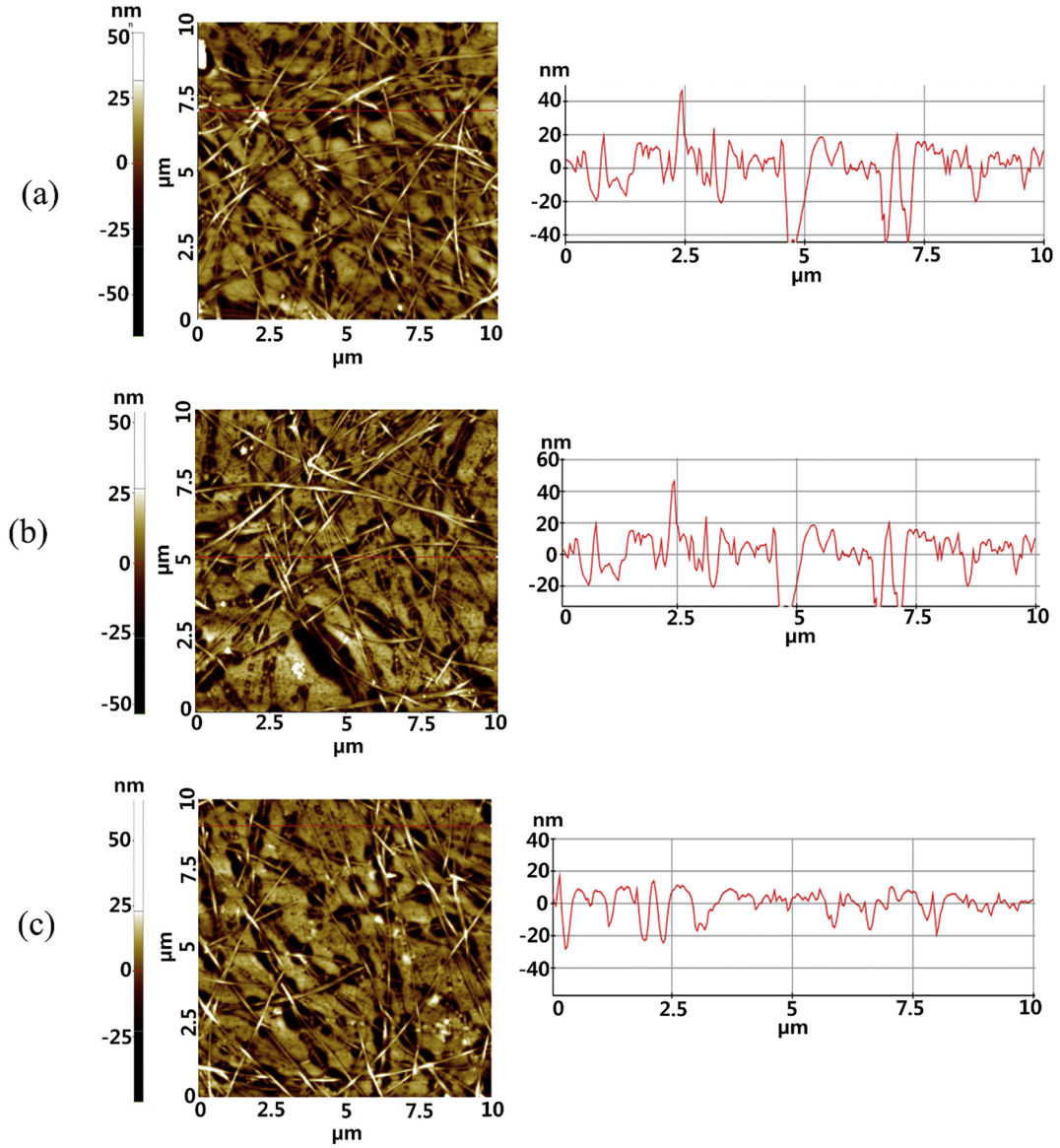

Fig. 4. AFM images of pristine (a) annealed AgNW/PET, (b) annealed AgNW/MM/PET and (c) hot pressed AgNW/MM/PET TCE.

Table 1
Roughness data of AgNW/PET and AgNW/MM/PET TCEs.

TCEs	RMS roughness (nm)	Max peak to valley (nm)
Annealed AgNW/PET	11	~ 48
Annealed AgNW/MM/PET	14	~ 41
Hot Pressed AgNW/MM/PET	8	~ 16

(c_4) show the tilt view images of the annealed and hot pressed AgNW/MM/PET TCEs. From these images, it is visually confirm that the hot pressed AgNW/MM/PET has a smoother surface than the annealed AgNW/MM/PET TCE.

The opto-electric performance of the AgNW/MM/PET TCE were studied by measuring the optical transmittance and the sheet resistance, respectively. Fig. 2 shows the comparison of the values of the sheet resistance and the optical transmittance of the annealed AgNW/PET, MM/PET, the annealed and hot pressed AgNW/MM/PET TCEs. The annealed AgNW/PET TCE displays 95.44% of transmittance with 38.12 Ω/sq. of sheet resistance. The MM/PET TCE exhibits 95.5% of transmittance and 18 Ω/sq. of sheet resistance, and the annealed AgNW/MM/PET TCE shows 0.740 Ω/sq. of sheet resistance with 90.1% transmittance. The sheet resistance of MM/PET TCE decreased from 18 to 0.740 Ω/sq. as the cavity between metal grid was filled by the AgNWs, as shown in Fig. 1(b_1). The hot pressed AgNW/MM/PET TCE shows 0.668 Ω/sq. of sheet resistance and 91.25% of transmittance, which were improved values compared to those of the annealed AgNW/MM/PET TCE. Due to the hot pressing, the nanowires, which were stacked on top of one another, tend to weld together and form a continuous pathway for the electric carriers (shown in Fig. 1(c_3) by circle). In case of annealed AgNW/MM/PET TCE sample, the nanowires were welded together by thermal heat, but there were still some imperfect junctions where multiple nanowires were stacked on top of one another (shown in Fig. 1(b_3) by arrow). Hence, the hot pressed AgNW/MM/PET TCE has excellent opto-electric performance make it useful for the fabrication of organic photovoltaic device, OLEDs, and solar cells [10,41]. Fig. 3 show the sheet resistance and the optical transmittance of the AgNW/MM/PET TCE that was pressed (10 MPa) at different temperatures. Fig. 3 shows that the AgNW/MM/PET TCE, which was pressed (10 MPa) at a temperature of 50 °C, demonstrated optimal opto-electric performance.

Atomic force microscopy (AFM) analysis were used to study the surface morphology of the fabricated TCEs. Fig. 4(a–c) shows AFM

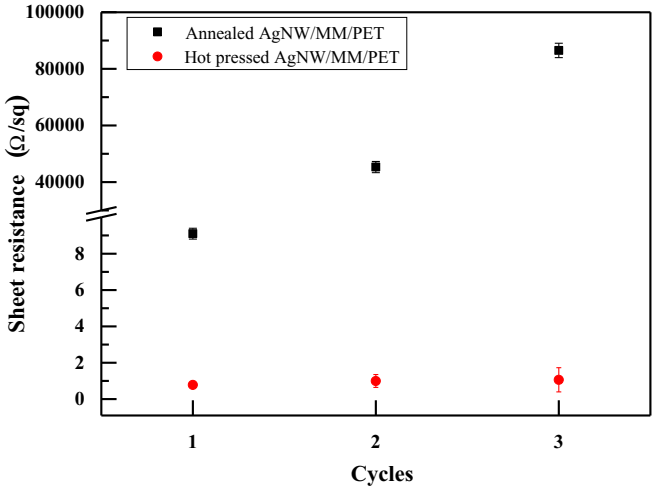

Fig. 5. Sheet resistances of TCE with the number of tape test.

images of the annealed AgNW/PET, annealed AgNW/MM/PET, and hot pressed AgNW/MM/PET TCEs. Table 1 summaries the RMS roughness and maximum peak-to-valley data. The root mean square roughness (Rq) and maximum peak-to-valley value for annealed AgNW/PET and AgNW/MM/PET TCEs were 11, 48 nm and 14, 41 nm, respectively. For hot pressed AgNW/MM/PET TCE, the Rq was dropped to 44% compare to annealed AgNW/MM/PET TCE. The Rq and maximum peak-to-valley value for hot pressed AgNW/MM/PET TCE were 8 and 16 nm, respectively. This outcome proves that by hot pressing process the Rq and max peak-to-valley value of AgNW/MM/PET TCE decrease without the use of additional materials. In addition, for a mentioned sheet resistance, the hot pressed AgNW/MM/PET TCE is more transparent than electrodes that use additional materials [25,42].The achieved surface roughness of the hot pressed AgNW/MM/PET TCE is favorable in organic electronic device applications. The scanned height shows that the wire was flattened by hot pressing, in a manner similar to the results seen Fig. 1(c_4).

The sheet resistance of the annealed and hot pressed AgNW/MM/PET TCEs after the tape test are shown in Fig. 5. The sheet resistance of the hot pressed AgNW/MM/PET TCE after three taping test cycle was increased up to 1.06 Ω/sq., which was only a 0.6% increment of the sheet resistance compared to the initial value. However, for the annealed Ag NW/MM/PET TCE, after three taping test cycles the sheet resistance increased to 86.5 KΩ/sq. Although the adhesion of AgNW is critical factor for electrical and mechanical properties, it is difficult to directly quantify the adhesion energy of nanowires using conventional peel test or 4 point bending test. However, in Fig. 5, the hot-pressed AgNW sample showed highly stable the sheet resistance change during tape testing which implies the improvement of adhesion of AgNW and enhancement of electrical and mechanical reliabilities. The hot pressed AgNW/MM/PET TCE sample also exhibited outstanding mechanical stability. To demonstrate this, the AgNW/MM/PET TCE sample fabricated on a flexible substrate was bent while the electrical resistance was measured in situ. Fig. 6(a) shows the resistance change of the annealed and hot pressed AgNW/MM/PET TCE samples as a function of the bending radius. Neither the annealed nor the hot pressed AgNW/MM/PET TCE samples showed an electrical resistance change until bending deformation occurred by bending in the radius of 2 mm, which corresponded to a bending strain, ε of 3%. However, in the annealed and hot pressed samples, a significant difference in long-term reliability was exhibited.

The electrical resistances of the AgNW/MM/PET TCE samples were measured during the bending fatigue test by repeated bending/unbending motions, as shown in Fig. 6(b). The bending radius of the bending fatigue test was 5 mm. The resistance of the annealed AgNW/MM/PET TCE sample increased to 12% after 1000 cycles, but that of the hot pressed sample increased only 6%, or half of the value of the annealed sample (Fig. 6(b)). Thermo-mechanical pressure between nanowires caused the AgNWs to form more stable junctions after hot press processing, as shown in Fig. 1. Also, the adhesion of the nanowires is improved by hot pressing, as illustrated in Fig. 5 [43]. This obtained result demonstrates that using simple and low cost thermo-mechanical pressure, we can improve the conductivity and mechanical stability of the nanowires, especially at the junctions, which are weakest points in the nanowire network, the hot pressed sample exhibited superior long-term mechanical reliability.

4. Conclusions

In this work, the AgNW/MM/PET hybrid TCE was fabricated with enhanced opto-electric property using the hot pressing method after the wire wound-rod coating prosess. We developed low-resistance TCE via hybridization of metal mesh and AgNWs, which also resulted in a smooth surface. Hot press facilitated effective hybridization of metal mesh and AgNWs without thermal or mechanical damage of pre-processed metal mesh and AgNWs electrodes. Fabricated hot-pressed AgNW/MM/PET TCE showed 0.668 Ω/sq. of sheet resistance along with 91.25% of transmittance at 550 nm. AgNW/MM/PET TCE was better to that of MM/PET or AgNW/PET due to the synergistic effect of the combination of microscale metal mesh and nanoscale nanowire. Additionally, a smooth surface of TCE was obtained by hot pressing. The achieved surface roughness and maximum peak-to-valley value of the hot pressed AgNW/MM/PET TCE was 8 and 16.33 nm, respectively. Furthermore, the hot pressed AgNW/MM/PET TCE exhibited excellent

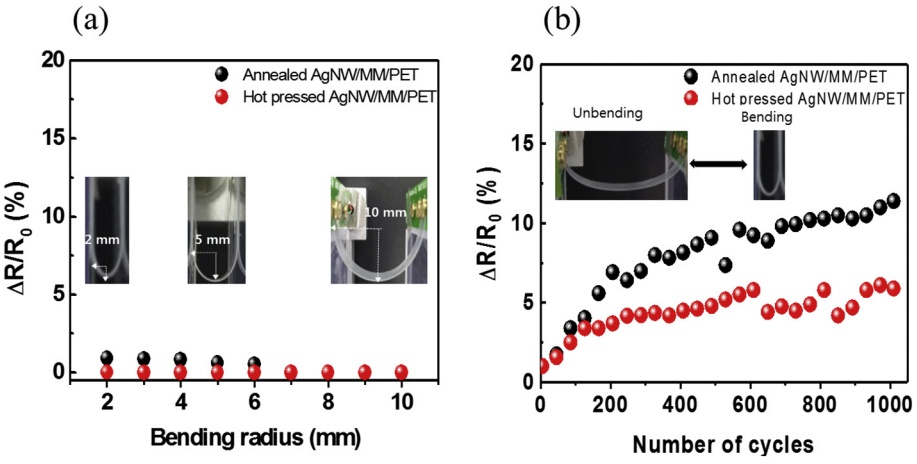

Fig. 6. (a) Electrical resistance change of annealed and hot pressed AgNW/MM/PET TCE sample as a function of the bending radius. Inset: Bending test of the flexible electrode by changing the gap between two boards. Nanowire samples were located on the inside of the bending shape. (b) Electrical resistance changes of annealed and hot pressed AgNW/MM/PET TCE samples as a function of the bending cycles with a bending radius of 5 mm.

mechanical stability, with strong adhesion as confirmed by both the bending test and the taping tests. The hot pressed AgNW/MM/PET electrodes with low surface roughness and outstanding opto-electrical properties are be a potential candidate to replace indium doped tin oxide electrodes in flexible electronic application.

Acknowledgements

This work was supported by the 2019 Yeungnam University Research Grant.

References

[1] W. Fu, L. Liu, K. Jiang, Q. Li, S. Fan, Super-aligned carbon nanotube films as aligning layers and transparent electrodes for liquid crystal displays, Carbon. 48 (2010) 1876–1879.
[2] J. Lee, P. Lee, H. Lee, D. Lee, S.S. Lee, S.H. Ko, Very long Ag nanowire synthesis and its application in a highly transparent, conductive and flexible metal electrode touch panel, Nanoscale. 4 (2012) 6408–6414.
[3] Y. Paska, T. Stelzner, O. Assad, U. Tisch, S. Christiansen, H. Haick, Molecular gating of silicon nanowire field-effect transistors with nonpolar analytes, ACS Nano 6 (1) (2012) 335–345.
[4] G.L. Brian, D.C. Paine, Applications and processing of transparent conducting oxides, MRS Bull. 25 (2000) 22–27.
[5] R.G. Gordon, Criteria for choosing transparent conductors, MRS Bull. 25 (2000) 52–57.
[6] P.B. Catrysse, S. Fan, Nanopatterned metallic films for use as transparent conductive electrodes in optoelectronic devices, Nano Lett. 10 (2010) 2944–2949.
[7] U. Bach, D. Lupo, P. Comte, J.E. Moser, F. Weissörtel, J. Salbeck, H. Spreitzer, M. Grätzel, Solid-state dye-sensitized mesoporous TiO_2 solar cells with high photon-to-electron conversion efficiencies, Nature. 395 (1998) 583–585.
[8] S. De, T.M. Higgins, P.E. Lyons, E.M. Doherty, P.N. Nirmalraj, W.J. Blau, J.J. Boland, J.N. Coleman, Silver nanowire networks as flexible, transparent, conducting films: extremely high DC to optical conductivity ratios, ACS Nano 3 (2009) 1767–1774.
[9] S.I. Kim, K.W. Lee, B.B. Sahu, J.G. Han, Flexible OLED fabrication with ITO thin film on polymer substrate, Jpn. J. Appl. Phys. 54 (2015) 13001–13004.
[10] Z. Chen, B. Cotterell, W. Wang, E. Guenther, S. Chua, A mechanical assessment of flexible optoelectronics device, Thin Solid Films 394 (2001) 201–205.
[11] A. Kumar, C. Zhou, The race to replace tin-doped indium oxide: which material will win? ACS Nano 4 (1) (2010) 11–14.
[12] S. Ju, J. Li, J. Liu, P. Chen, Y. Ha, F. Ishikawa, H. Chang, C. Zhou, A. Facchetti, D.B. Janes, T.J. Marks, Transparent active matrix organic light-emitting diode displays driven by nanowire transistor circuitry, Nano Lett. 8 (4) (2008) 997–1004.
[13] M.A. Shinde, K. Mallikarjuna, J.S. Noh, H.K. Kim, Highly stable silver nanowires based bilayered flexible transparent conductive electrode, Thin Solid Films 660 (2018) 447–454.
[14] J. Wang, J. Jiu, M. Nogi, A highly sensitive and flexible pressure sensor with electrodes and elastomeric interlayer containing silver nanowires, Nanoscale. 7 (2015) 2926–2932.
[15] J. Wang, J. Jiu, T. Araki, Silver nanowire electrodes: conductivity improvement without post-treatment and application in capacitive pressure sensors, Nano-Micro Lett. 7 (1) (2015) 51–58.
[16] M.A. Shinde, H.K. Kim, Flexible electrochromic device with simple solution processed stable silver nanowire based transparent conductive electrodes, Synth. Met. 254 (2019) 97–105.
[17] G. Gruner, Carbon nanotube films for transparent and plastic electronics, J. Mater. Chem. 16 (2006) 3533–3539.
[18] K.S. Kim, Y. Zhao, H. Jang, S.Y. Lee, J.M. Kim, K.S. Kim, J. Ahn, P. Kim, J. Choi, B.H. Hong, Large-scale pattern growth of graphene films for stretchable transparent electrodes, Nature. 457 (2009) 706–710.
[19] A. Elschner, W. Lövenich, Solution-deposited PEDOT for transparent conductive applications, MRS Bull. 36 (10) (2011) 794–798.
[20] J. Groep, P. Spinelli, A. Polman, Transparent conducting silver nanowire networks, Nano Lett. 12 (2012) 3138–3144.
[21] J. Zou, H. Yip, S.K. Hau, A.K.Y. Jen, Metal grid/conducting polymer hybrid transparent electrode for inverted polymer solar cells, Appl. Phys. Lett. 96 (2010) 203301–203303.
[22] D.S. Hecht, L. Hu, G. Irvin, Emerging transparent electrodes based on thin films of carbon nanotubes, graphene, and metallic nanostructures, Adv. Mater. 23 (2011) 1482–1513.
[23] J.H. Park, D.Y. Lee, Y. Kim, J.K. Kim, J.H. Lee, J.H. Park, T. Lee, J.H. Cho, Flexible and transparent metallic grid electrodes prepared by evaporative assembly, ACS Appl. Mater. Interfaces 6 (2014) 12380–12387.
[24] H.J. Kim, S.H. Lee, J. Lee, E.S. Lee, J.H. Choi, J.H. Jung, J.Y. Jung, D.G. Choi, High-durable AgNi nanomesh film for a transparent conducting electrode, Small. 10 (18) (2014) 3767–3774.
[25] Z. Yu, Q. Zhang, L. Li, Q. Chen, X. Niu, J. Liu, Q. Pei, Highly flexible silver nanowire electrodes for shape-memory polymer light-emitting diodes, Adv. Mater. 23 (2011) 664–668.
[26] D.Y. Choi, H.W. Kang, H.J. Sung, S.S. Kim, Annealing-free, flexible silver nanowire-polymer composite electrodes via a continuous two-step spray-coating method, Nanoscale. 5 (2013) 977–983.
[27] J.Y. Lee, S.T. Connor, Y. Cui, P. Peumans, Solution-processed metal nanowire mesh transparent electrodes, Nano Lett. 8 (2008) 689–692.
[28] D.S. Leem, A. Edwards, M. Faist, J. Nelson, D.D.C. Bradley, J.C. Mello, Efficient organic solar cells with solution-processed silver nanowire electrodes, Adv. Mater. 23 (2011) 4371–4375.
[29] J. Krantz, M. Richter, S. Spallek, E. Spiecker, C.J. Brabec, Solution-processed metallic nanowire electrodes as indium tin oxide replacement for thin-film solar cells, Adv. Funct. Mater. 21 (2011) 4784–4787.
[30] S. Jung, S. Lee, M. Song, D. Kim, D.S. You, J.K. Kim, C.S. Kim, T.M. Kim, K.H. Kim, J.J. Kim, J.W. Kang, Extremely flexible transparent conducting electrodes for organic devices, Adv. Energy Mater. 4 (2014) 1300474.
[31] X.Y. Zeng, Q.K. Zhang, R.M. Yu, C.Z. Lu, A new transparent conductor: silver nanowire film buried at the surface of a transparent polymer, Adv. Mater. 22 (2010) 4484–4488.
[32] T. Tokuno, M. Nogi, M. Karakawa, J. Jiu, T.T. Nge, Y. Aso, K. Suganuma, Fabrication of silver nanowire transparent electrodes at room temperature, Nano Res. 4 (2011) 1215–1222.
[33] T.C. Hauger, S.M.I. Al-Rafia, J.M. Buriak, Rolling silver nanowire electrodes: simultaneously addressing adhesion, roughness, and conductivity, ACS Appl. Mater. Interfaces 5 (2013) 12663–12671.
[34] Y.Y. Yu, Y.J. Ting, C.L. Chung, T.W. Tsai, C.P. Chen, Comprehensive study on chemical and hot press-treated silver nanowires for efficient polymer solar cell application, Polymers. 9 (2017) 635.
[35] T.L. Chen, D.S. Gosh, V. Mkhitaryan, V. Pruneri, Hybrid transparent conductive film on flexible glass formed by hot-pressing graphene on a silver nanowire mesh, ACS Appl. Mater. Interfaces 5 (2013) 11756–11761.
[36] L. Hu, H.S. Kim, J.Y. Lee, P. Peumans, Y. Cui, Scalable coating and properties of transparent, flexible, silver nanowire electrodes, ACS Nano 4 (2010) 2955–2963.
[37] C.H. Liu, X. Yu, Silver nanowire-based transparent, flexible, and conductive thin film, Nanoscale Res. Lett. 6 (2011) 75.
[38] D.G. Khim, H. Han, K.J. Baeg, J.W. Kim, S.W. Kwak, D.Y. Kim, Y.Y. Noh, Simple bar-coating process for large-area, high-performance organic field-effect transistors and ambipolar complementary integrated circuits, Adv. Mater. 25 (2013) 4302–4308.
[39] B.J. Kim, H.A.S. Shin, S.Y. Jung, Y. Cho, O. Kraft, I.S. Choi, Y.C. Joo, Crack nucleation during mechanical fatigue in thin metal films on flexible substrates, Acta Mater. 61 (2013) 3473–3481.
[40] B.J. Kim, H.A.S. Shin, J.H. Lee, T.Y. Yang, T. Haas, P.A. Gruber, I.S. Choi, O. Kraft, Y.C. Joo, Effect of film thickness on the stretchability and fatigue resistance of Cu films on polymer substrates, J. Mater. Res. 29 (2014) 2827–2834.
[41] S. Coskun, E.S. Ates, H.E. Unalan, Optimization of silver nanowire networks for polymer light emitting diode electrodes, Nanotechnology. 24 (2013) 125202.
[42] W. Gaynor, G.F. Burkhard, M.D. McGehee, P. Peumans, Smooth nanowire/polymer composite transparent electrodes, Adv. Mater. 23 (2011) 2905–2910.
[43] H.H. Khaligh, I.A. Goldthorpe, Hot-rolling nanowire transparent electrodes for surface roughness minimization, Nanoscale Res. Lett. 9 (2014) 310.